Aspects of the Verwey transition in magnetite

Hitoshi Seo,[1] Masao Ogata,[2] and Hidetoshi Fukuyama[3]

[1]*Correlated Electron Research Center (CERC), National Institute of Advanced Industrial Science and Technology (AIST), Ibaraki 305-8562, Japan*
[2]*Department of Physics, University of Tokyo, Tokyo 113-0033, Japan*
[3]*Institute for Solid State Physics, University of Tokyo, Chiba 277-8581, Japan*

A mechanism of the Verwey transition in magnetite (Fe_3O_4), which has been argued to be a charge ordering transition so far, is proposed. Based on mean-field calculations for a three-band model of spinless fermions appropriate for d electrons of Fe ions in B sites, it is indicated that the phase transition should be a bond dimerization due to the cooperative effects of strong electronic correlation and electron-phonon interaction. The results show that the ferro-orbital ordered state is stabilized in a wide temperature range due to the strong on-site Coulomb interaction between different t_{2g} orbitals, resulting in an effectively one-dimensional electronic state, which leads the system toward an insulating state through a Peierls lattice distortion with a period of two Fe(B) ions, i.e., bond dimerization. Furthermore, it is found that the interplay between such lattice distortions in Fe(B) ions, and the lattice elastic energy of Fe(B)-O as well as Fe(A)-O bonds, gives rise to a competition between two different three-dimensional patterns for the bond dimerization, and can stabilize a complicated one with a large unit-cell size. The results are compared with the known experimental facts.

PACS number(s): 71.30.+h, 71.10.Fd, 71.10.Hf, 75.50.Gg

I. INTRODUCTION

The nature of the Verwey transition in magnetite (Fe_3O_4) has not yet been clarified, in spite of intensive studies from very early days.[1] Fe_3O_4 forms a cubic spinel structure, as shown in Fig. 1, where one-third of the Fe ions occupy the A sites, tetrahedrally coordinated by four oxygen ions, while the remaining two-thirds are octahedrally surrounded by six oxygen ions, which are the B sites. One can see that Fe(B)$_2$O$_4$ layers and Fe(A) layers are stacked alternately, while the z axis can be taken as any of the three cubic crystal axes. Although the primitive cell is a rhombohedral parallelepiped containing two formula units of Fe_3O_4, the unit cell is conveniently chosen as the cubic one, as shown in Fig. 1, containing eight formula units to which we also refer in this paper.

The Fe(A) ions are trivalent, while the Fe(B) ions are mixed valent with a formal average valence Fe(B)$^{2.5+}$. Below $T_N = 858$ K, the magnetic moments of the Fe ions are ferrimagnetically ordered, where the A and B sites have opposite spin directions, with d-orbital occupations represented as $(t_{2g\uparrow})^3 (e_{g\uparrow})^2$ and $(t_{2g\downarrow})^3 (e_{g\downarrow})^2 (t_{2g\uparrow})^{0.5}$, respectively. Well below T_N, an abrupt increase in the resistivity takes place at $T_V \simeq 120$ K, which is now called after Verwey, who discovered it[2] and proposed that the phenomenon is due to the ordering of equal numbers of Fe^{2+} and Fe^{3+} on the B sites, i.e., charge ordering (CO) among the "extra" $t_{2g\uparrow}$ electrons.[3]

As for theoretical studies of this phenomenon, the electronic properties of the spin-polarized $t_{2g\uparrow}$ electrons were investigated frequently by a single-band spinless fermion model on the B sites originally proposed by Cullen and Callen.[4,5] Such a picture of spinless fermion proved to be valid by band-structure calculations,[6–8] where the majority spin ($\downarrow$) band of the Fe(B) ions is shown to be fully occupied and the Fermi energy crosses the minority spin ($\uparrow$)

band. In the model of Cullen and Callen the triple degeneracy of the t_{2g} orbitals was neglected, so that the band is half-filled, corresponding to half a charge per site as in the actual compound. This model is investigated within the Hartree approximation where the ground state shows a phase transition from a metallic state to a CO state as the intersite Coulomb interaction V_{ij} is increased,[4] providing the most
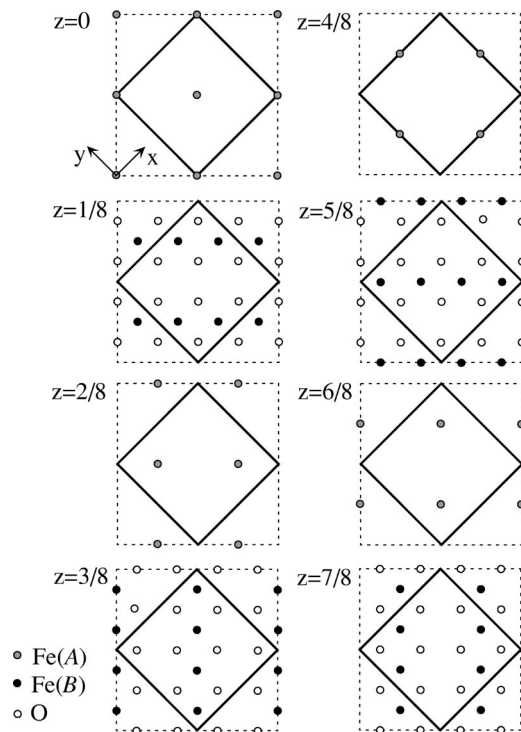
FIG. 1. Cubic spinel structure of Fe_3O_4. The thick square shows the cubic unit cell with a lattice constant a in the xy plane, while the z coordinates are indicated by the fraction of a. The unit cell in the xy plane for $T < T_V$ is shown by the dotted line.

naive picture for the CO state in the magnetite.

However, no CO pattern so far considered has been successful in presenting a satisfactory interpretation for the known experiments, including the one originally proposed in Ref. 3 and other more complicated patterns.[9,10] In addition, the expected short-range fluctuation of the CO due to the frustration in V_{ij},[11] arising from the fact that the network connecting the Fe(B) ions forms a coupled tetrahedra system, is not found either in neutron-scattering[12] or resonant x-ray scattering measurements.[13] Furthermore, recent NMR[14] and x-ray anomalous scattering[15] experiments for $T < T_V$ even cast doubts on the existence of CO. Todo $et\ al.$,[16] based on these suggestions and their finding of a pressure-induced metallic ground state above 8 GPa, proposed that the low-temperature phase below T_V may be a kind of "Mott insulator" where the B sites are forming dimers due to orbital ordering (OO).

This idea of the Mott insulating state resembles that in low-dimensional quarter-filled organic conductors theoretically studied by Kino and the present authors,[17] where the fact that there exists one carrier per two sites is the same as that for the B sites in Fe_3O_4. In such organic conductors, the Mott insulating state can be understood from the viewpoint that each charge localizes in every two sites, i.e., dimer. The dimerization is either due to the anisotropy in the transfer integrals from the lattice structure,[18] or due to the spontaneous formation of bond dimerization (BD) by the electron-phonon interaction where the one-dimensionality plays a crucial role.[19]

In this paper, we will show that this latter type of insulating state with BD can actually emerge in Fe_3O_4, and propose it to be the mechanism of the Verwey transition in this compound. In Sec. II we will discuss how the strong correlation among electrons stabilizes an OO state with an effectively one-dimensional (1D) electronic structure, and how additional electron-phonon interaction can give rise to a BD state. Moreover, discussions in Sec. III of the elastic lattice energy of the whole system will lead to the three-dimensional pattern of this BD expected below T_V. The relevance of our proposal to the experimental facts is discussed in Sec. IV, and the conclusion is given in Sec. V.

II. BOND DIMERIZATION ON B SITES

A. Three-band model

We start with the model of Mishra $et\ al.$,[20] who extended the spinless fermion model of Cullen and Callen[4] by including the triple degeneracy of t_{2g} orbitals appropriate for B sites in Fe_3O_4. The Hamiltonian is written as

$$H = \sum_{\langle ij \rangle} \sum_{\mu\nu} t_{ij}^{\mu\nu} c_{i\mu}^{\dagger} c_{j\nu} + \sum_{i} \sum_{\mu \neq \nu} U n_{i\mu} n_{i\nu} + \sum_{\langle ij \rangle} V n_i n_j,$$

(1)

where $c_{i\mu}^{\dagger}$ ($c_{i\mu}$) and $n_{i\mu}$ denote the creation (annihilation) and number operators of the electron at the ith site of orbital μ, respectively, where the orbital indices take xy, yz, or
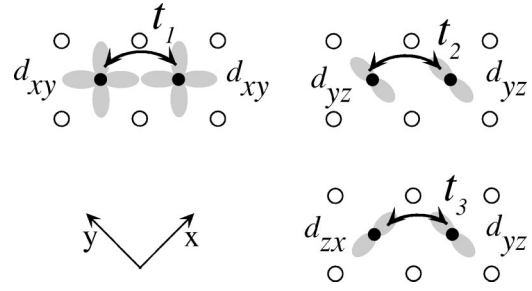
FIG. 2. A schematic representation of the transfer integrals between neighboring B site pairs in the xy plane with different orbital occupations. The simultaneous cyclic substitution of the orbital indices and the axes of coordinates, $x \rightarrow y, y \rightarrow z, z \rightarrow x$ or $x \rightarrow z, y \rightarrow x, z \rightarrow y$, also provide the three transfer integrals, while for the other configurations are $t_{ij}^{\mu\nu} = 0$.

zx.[21] n_i is the number operator for each site, i.e., $n_i = n_{ixy} + n_{iyz} + n_{izx}$, and $\langle ij \rangle$ denotes the nearest-neighbor site pair along the coupled Fe(B) ion tetrahedra network. U and V are the on-site Coulomb energy between different orbitals (note that the same orbital cannot be doubly occupied) and the nearest-neighbor Coulomb energy, respectively. By using the transfer integrals for $\langle ij \rangle$ pairs calculated in Ref. 7, $t_{dd\sigma} = -0.41$ eV, $t_{dd\pi} = 0.054$ eV, and $t_{dd\delta} = 0.122$ eV, the three kinds of transfer integrals $t_{ij}^{\mu\nu}$, with different configurations of orbital occupations, as shown in Fig. 2, can be estimated[22] as $t_1 = 3t_{dd\sigma}/4 + t_{dd\delta}/4 = -0.278$ eV, $t_2 = t_{dd\pi}/2 + t_{dd\delta}/2 = 0.085$ eV, and $t_3 = t_{dd\sigma}/2 - t_{dd\delta}/2 = -0.035$ eV, where the notations of t_{1-3} are given in Fig. 2.

Mishra $et\ al.$ treated the Coulomb interaction terms U and V by means of a Hartree mean-field approximation

$$n_{i\mu} n_{j\nu} \rightarrow \langle n_{i\mu} \rangle n_{j\nu} + n_{i\mu} \langle n_{j\nu} \rangle - \langle n_{i\mu} \rangle \langle n_{j\nu} \rangle,$$

(2)

and determined the ground state of the system. Their results for a case with a fixed value of $U = 4.0$ eV, relevant for magnetite,[7] showed that the CO state is stabilized in the ground state for $V > V_c = 0.38$ eV,[23] while the metallic state is stabilized for $V < V_c$, qualitatively the same as in the one-band model;[4] these authors concluded that the former state is relevant for the magnetite.

Although not emphasized in Ref. 23, every site is almost fully occupied by the same orbital state, that is, ferro-OO is realized in both of these states due to the large value of U. The three d_{xy}-, d_{yx}- and d_{yz}-OO states are energetically degenerate, and the electronic structure becomes one-dimensional once one of the OO state is realized, which is particular to the spinel structure. For example the d_{xy}-OO state has 1D arrays of sites connected by the largest transfer integral t_1, which are along the [110] and [1$\bar{1}$0] directions for xy planes with z coordinates $z = (4n+1)/8$ and $z = (4n+3)/8$, respectively (see Fig. 1).

In a metallic state with the presence of this d_{xy}-OO, the expectation values of the charge density for all sites are $\langle n_{ixy} \rangle \simeq 0.5$ and $\langle n_{iyz} \rangle = \langle n_{izx} \rangle \simeq 0$. As for the CO state, i.e., the coexistent state of OO and CO, planes with 1D arrays of

$\langle n_{ixy} \rangle \simeq 0.5 + \delta$ and those with $\langle n_{ixy} \rangle \simeq 0.5 - \delta$, corresponding to Fe^{2+} and Fe^{3+}, respectively, are stacked alternatively along the z direction, where the CO pattern is the one proposed by Verwey. Here δ is the amount of charge disproportionation, which rapidly increases as the value of V is increased from V_c, and reaches around 0.9 for $V = 1.0$ eV. The other two d_{yz} and d_{zx} orbitals are also almost empty in the CO state.

In contrast to conclusion of Mishra *et al.* that this CO state is realized in magnetite, recent experimental proposals of the absence of CO, mentioned in Sec. I, suggest that the former *OO metallic* state should be relevant to the actual system, and that the origin of the insulator is other than CO. The destabilization of the CO state may be due to the screening of the long-range Coulomb interaction and/or the effect of frustration among V_{ij} mentioned above.[11] Actually, the melting of CO due to frustration among V_{ij}'s was demonstrated theoretically in 1D systems,[24] though we will not discuss such possibilities in magnetite further in this paper. Here we will concentrate on how the OO metallic state shows instability toward an insulating state, and its possible consequence on the lattice structure in this insulating phase.

B. Peierls instability in an orbital ordered state

In the following we consider the case of the d_{xy}-OO metallic state. The properties of this ferro-OO state can be extracted by an effective noninteracting 1D spinless fermion system, $H_{1D} = \Sigma_l t_1 (c_l^\dagger c_{l+1} + \text{H.c.})$ with a half-filled band, l being the site index along the 1D directions [110] or [1$\bar{1}$0]. This model should be valid for $U \gg t_1 \gg t_2, t_3$ in Eq. (1), with $V_{ij} = 0$. It is well known that such a half-filled 1D band has a Peierls instability with a wavelength two times the interatomic distance,[19] i.e., an *instability toward the BD state*. This will alternate the atomic displacements along the 1D direction, resulting in an alternation in the transfer integrals as $t_1 \rightarrow t_1(1 + (-1)^l u)$, where u represents the degree of BD. Actually the system can be mapped onto the $S = 1/2$ XY chain via a Jordan-Wigner transformation, so that our metallic state here corresponds to the spin liquid state, which shows an instability toward the spin Peierls-state, that is, the BD state in spin system. Thus, once electron-phonon interaction is present, the OO state in magnetite will undergo a BD transition to gain kinetic energy by making a gap at the band center, resulting in an *insulating* state. We propose this scenario to be the origin of the insulating ground state of magnetite, Fe_3O_4. Such a state will be realized if it is not destroyed by the interchain interactions t_2 and t_3, which is investigated in Sec. II C.

We should note that this Peierls instability is different from the usual one in a 1D electron system of weak coupling, since the assumption of the spinless fermion here is due to the ferrimagnetic spin ordering realized in the limit of infinite value of on-site *intra*orbital Coulomb interaction. One may say that the BD state here is rather analogous to the Mott insulator in quarter-filled compounds noted in Sec. I, where the origin is also the interplay between the strong on-site Coulomb interaction and the dimerization.[18] Actually the minimal model for such compounds, i.e., a one-band
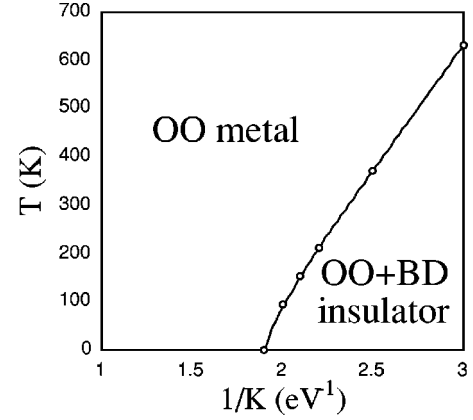
FIG. 3. Mean-field phase diagram of the three-band Peierls-Hubbard model for B sites, on the plane of temperature T, and the inverse of the lattice elastic coupling constant, $1/K$. OO and BD represent orbital-ordering and bond dimerization, respectively.

Hubbard model of quarter-filling with dimerization in the transfer integrals,[17] is mapped in the limit of infinite values of on-site Coulomb interactions onto a half-filled spinless fermion model with dimerized transfer integrals,[19] where the Mott insulating state in the former model corresponds to the BD state in the latter.

C. Peierls-Hubbard model

To investigate the stability of the BD state in an actual three-dimensional system, we include the lattice degree of freedom by adding a Peierls-type coupling to Eq. (1), i.e., we treat the Peierls-Hubbard (PH) model for magnetite. This is expressed as

$$H_{PH} = \sum_{\langle ij \rangle} \sum_{\mu\nu} t_{ij}^{\mu\nu} (1 + u_{ij}) c_{i\mu}^\dagger c_{j\nu}$$
$$+ \sum_i \sum_{\mu \neq \nu} U n_{i\mu} n_{i\nu} + \sum_i \frac{1}{2} K u_{ij}^2, \qquad (3)$$

where u_{ij} and K are the lattice distortion between a nearest-neighbor site pair $\langle ij \rangle$ and the coupling constant for the elastic energy, respectively. The intersite Coulomb interaction term is neglected here since it is not relevant in our discussion, as mentioned in Sec. II A. The on-site Coulomb interaction term U is treated within the mean field approximation, as in Eq. (2), and self-consistent solutions are obtained. We restrict ourselves to the case of $u_{ij} = (-1)^l u$ associated with the three kinds of transfer integrals along the [110] and [1$\bar{1}$0] directions and to $u_{ij} = 0$ for the other directions. This provides the BD state discussed in Sec. II B, u being the degree of BD, and the value of u is determined for each choice of parameters so as to minimize the energy. We note that the calculated energy does not depend on different BD patterns, since the effect of the lattice distortion on the lattice elastic energy and on the transfer integrals is restricted in each chains.
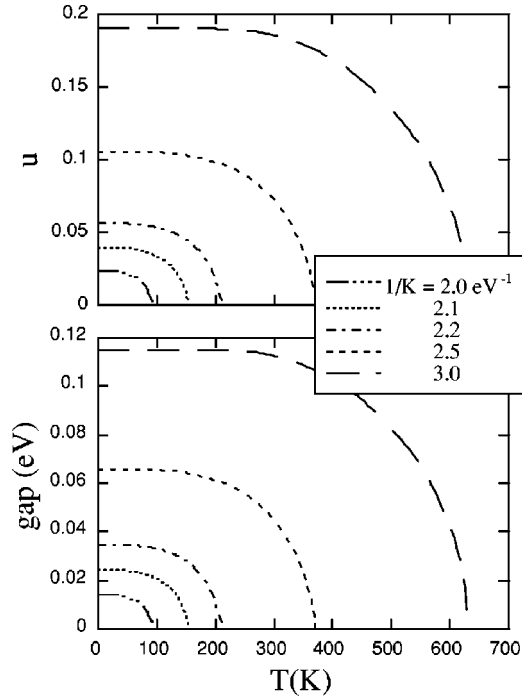
FIG. 4. Temperature dependences of the degree of BD, u, and the band gap for several values of $1/K$.

The results show that the BD state can actually be stabilized when $1/K$ exceeds a critical value. In Fig. 3, the obtained phase diagram within the finite-temperature mean-field approximation is shown for the case of fixed U $=4.0$ eV, the same as in the calculation of Mishra et al.[20] mentioned in Sec. II A. The ground state is OO metallic with $u=0$ below $1/K<1.9$ eV^{-1}, whereas the OO state with u $\neq 0$, i.e., the BD state, is stabilized for $1/K>1.9$ eV^{-1}, where the system is insulating. Below $T_{OO} \simeq 6000$ K, which is well above the temperature range shown in Fig. 3, ferro-OO is present, and the para-orbital state is stabilized only above T_{OO}.

The optimized value of u and the band gap in the BD state are plotted as functions of T in Fig. 4. It can be seen that the lattice dimerization and the band gap decrease as the temperature is increased, and vanish continuously at $T=T_c$, showing a second-order insulator-to-metal phase transition. On the other hand, the charge density for each orbital state does not change noticeably from $\langle n_{ixy} \rangle \simeq 0.5$ and $\langle n_{iyz} \rangle$ $=\langle n_{izx} \rangle \simeq 0$, for all sites in the temperature range with which we are concerned. In other words, the OO is not affected through the metal-insulator transition.

III. BOND DIMERIZATION PATTERN

The three-dimensional BD pattern in the actual compound cannot be determined by the preceding calculation alone, since the calculated energy does not depend on the interchain configuration, as mentioned above. To discuss the stability of different BD states theoretically, the lattice elastic energy

should be the most important factor, since the BD produces large lattice distortion so that it moderately affects the lattice energy. The influence of the BD on the the interchain transfer integrals is small, so the difference in the kinetic energy between different BD states is neglected in the following discussion.

The lattice elastic energy in Fe$_3$O$_4$, $\mathcal{E}_{lat}$, can be estimated by the sum of $(K/2)(\Delta u)^2$ for all nearest-neighbor Fe-O bonds, where Δu is the deviation of the Fe-O distance from that in the equilibrium position above T_V and K is the elastic constant. The value of K should take common values K_A for the Fe(A)-O bonds and K_B for the Fe(B)-O bonds, since all the Fe(A)-O bonds as well as Fe(B)-O bonds are crystallographically equivalent above T_V. Thus $\mathcal{E}_{lat}$ can be expressed as $\mathcal{E}_{A lat} + \mathcal{E}_{B lat}$ for Fe(A)-O and Fe(B)-O bonds, respectively, where

$$\mathcal{E}_{A lat} = \sum \frac{K_A}{2} (\Delta u_{A\text{-}O})^2, \tag{4}$$

$$\mathcal{E}_{B lat} = \sum \frac{K_B}{2} (\Delta u_{B\text{-}O})^2, \tag{5}$$

where $\Delta u_{A\text{-}O}$ and $\Delta u_{B\text{-}O}$ are Δu for the Fe(A)-O and Fe(B)-O bonds, respectively.

Then, as will be explained in detail below, there are two candidates for the BD states costing much less elastic energy than the others, as shown schematically in Figs. 5(a) and 5(b). In the former the dimerization pattern between adjacent 1D chains in the xy plane is in phase; thus we call this the in-phase BD state, where the unit cell is unchanged from a cubic unit cell above T_V. On the other hand, in the latter pattern the BD is antiphase, which is called antiphase BD state in the following. Here the unit cell becomes large as $\sqrt{2} \times \sqrt{2} \times 2$ of the cubic cell, as shown in Fig. 5. We will see below that a competition between two BD states arises depending on the relative value of K_A and K_B, and our proposal is that the antiphase BD pattern is realized in the actual compound.

To see this competition, let us calculate a semiphenomenological Landau-type free energy by taking into account both in phase and antiphase BD states. We consider the amount of lattice distortion for the BD in the Fe(B) ions to be uniform along each chain, denoted by u_1 and u_2, for alternate chains in the xy planes. Then the in-phase BD is characterized by $u_1=u_2$, while the antiphase BD is characterized by $u_1=-u_2$, as shown in Figs. 6(a) and 6(b), respectively. The motions of oxygens are approximated to be perpendicular to the chains in the xy planes, parametrized by u_{O1} and u_{O2}, for the chains with BD's of u_1 and u_2, respectively. Within these approximations, the Fe(A) ions all become crystallograhpically equivalent, and we allow their motions in any direction, thus represented by the x, y, and z components of the displacement vectors, u_{Ax}, u_{Ay}, and u_{Az}, respectively (see Fig. 6).

Then the free energy per formula unit of Fe$_3$O$_4$, $\mathcal{F}$, can be computed, where there are four Fe(A)-O bonds for $\mathcal{E}_{A lat}$ and 12 Fe(B)-O bonds for $\mathcal{E}_{B lat}$, as

(a) in-phase BD state

(b) anti-phase BD state
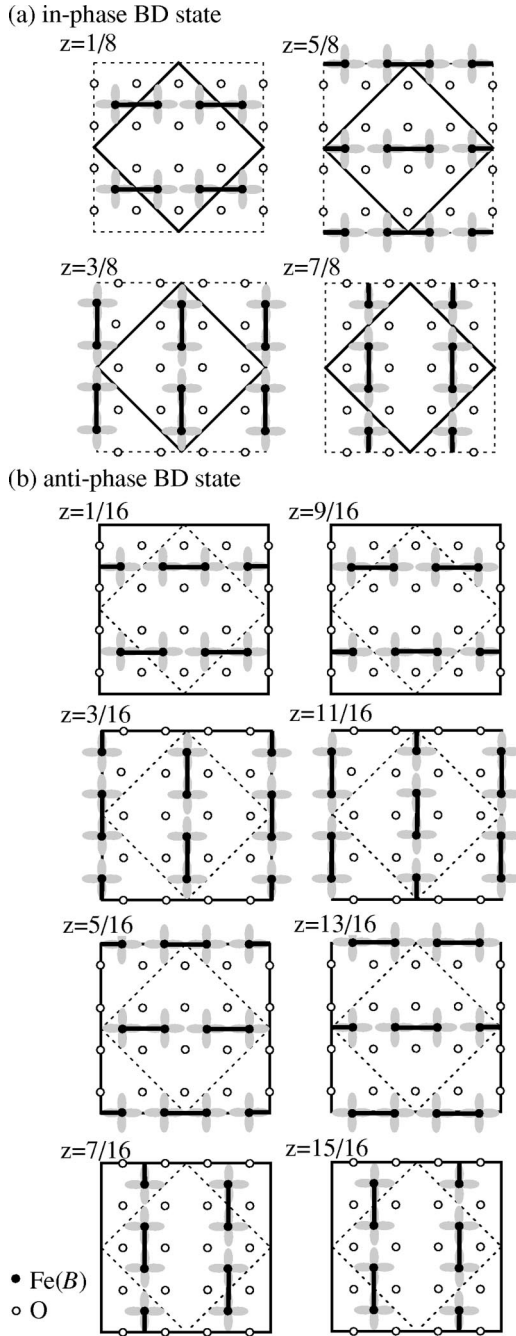
FIG. 5. Schematic representation of (a) the in phase BD state and (b) the antiphase BD state, both coexisting with the d_{xy}-OO. Only the $Fe(B)_2O_4$ layers are shown, where the thick $Fe(B)$-$Fe(B)$ bonds represent the dimers. The thick squares show the unit cell in the xy plane, and the z coordinates indicate the fraction of unit-cell size along the z direction. The unit-cell remains unchanged from the cubic one above T_V shown in Fig. 1 for the in phase BD pattern, while it becomes $\sqrt{2} \times \sqrt{2} \times 2$ of that for the antiphase BD pattern.

FIG. 6. Schematic representation of the ionic displacements in (a) the in phase BD pattern and (b) the antiphase BD pattern. Only two $Fe(B)_2O_3$ and $Fe(A)$ layers each are shown, and the directions of displacement are represented by arrows. The motions of the A sites in (a) which are along the z direction, are not shown.

$$\mathcal{F} = \mathcal{F}_{BD} + \mathcal{E}_{A\text{lat}} + \mathcal{E}_{B\text{lat}}, \qquad (6)$$

$$\mathcal{F}_{BD} = \alpha(T - T_c)(u_1^2 + u_2^2), \qquad (7)$$

$$\mathcal{E}_{A\text{lat}} = \frac{K_A}{2} \Biggl\{ \Biggl[\sqrt{u_{Ax}^2 + \left(\frac{1}{\sqrt{2}} + u_{Ay} - u_{O1}\right)^2 + \left(\frac{1}{2} + u_{Az}\right)^2} - \sqrt{\frac{3}{4}} \Biggr]^2$$
$$+ \Biggl[\sqrt{u_{Ax}^2 + \left(\frac{1}{\sqrt{2}} - u_{Ay} + u_{O2}\right)^2 + \left(\frac{1}{2} + u_{Az}\right)^2} - \sqrt{\frac{3}{4}} \Biggr]^2$$
$$+ \Biggl[\sqrt{\left(\frac{1}{\sqrt{2}} - u_{Ax} + u_{O1}\right)^2 + u_{Ay}^2 + \left(\frac{1}{2} - u_{Az}\right)^2} - \sqrt{\frac{3}{4}} \Biggr]^2$$
$$+ \Biggl[\sqrt{\left(\frac{1}{\sqrt{2}} + u_{Ax} - u_{O2}\right)^2 + u_{Ay}^2 + \left(\frac{1}{2} - u_{Az}\right)^2} - \sqrt{\frac{3}{4}} \Biggr]^2 \Biggr\}, \qquad (8)$$

(a) $K_A = 0.1$, $K_B = 0.3$ (b) $K_A = 0.5$, $K_B = 0.3$
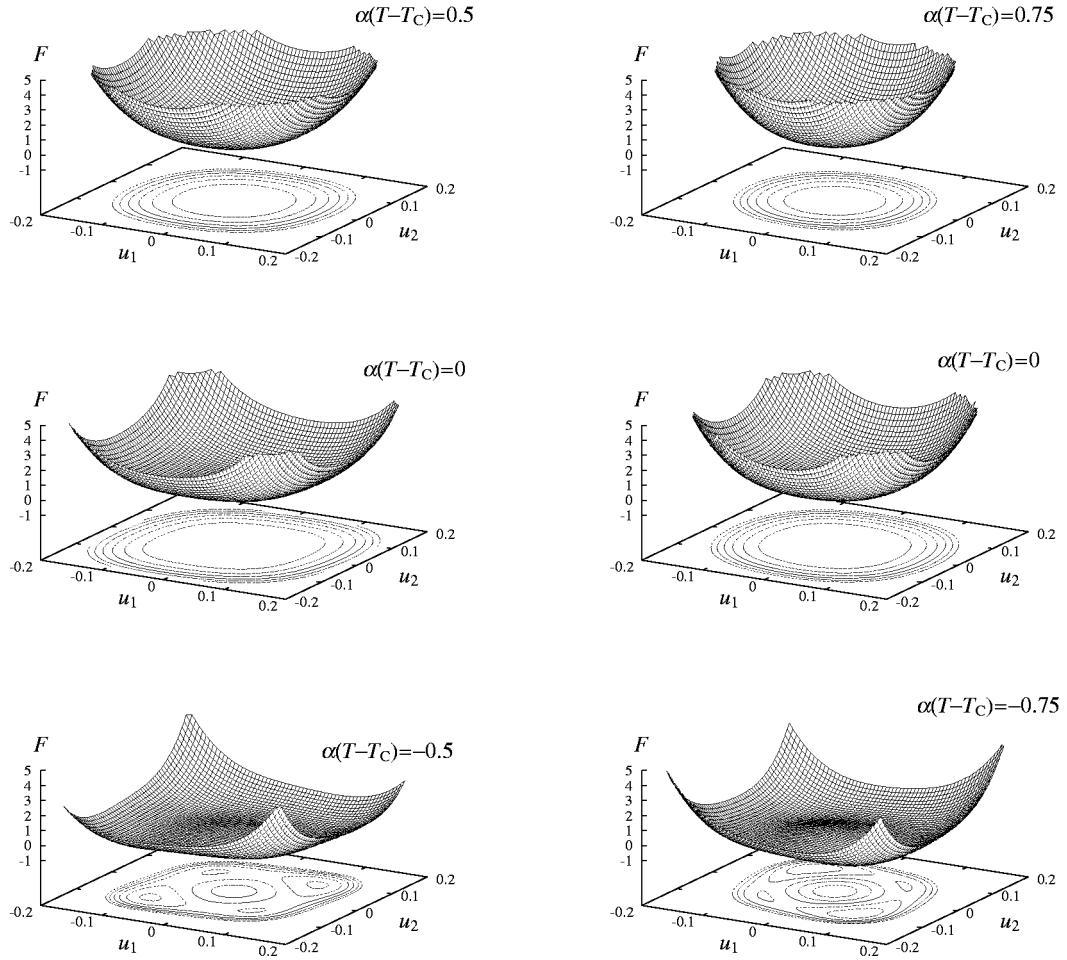
FIG. 7. Calculated free energy $\mathcal{F}$ for (a) $K_A = 0.1, K_B = 0.3$, and (b) $K_A = 0.5, K_B = 0.3$ at several temperatures, as a function of the degree of dimerization for adjacent chains, (u_1, u_2). Note that the contour plot in the base is guide for eyes.

$$
\mathcal{E}_{B\mathrm{lat}} = \frac{K_B}{2}\left\{ 2\left[\sqrt{\left(\frac{1}{\sqrt{2}} - u_1\right)^2 + \left(\frac{1}{\sqrt{2}} + u_{O1}\right)^2} - 1 \right]^2 \right.
$$

$$
+ 2\left[\sqrt{\left(\frac{1}{\sqrt{2}} - u_2\right)^2 + \left(\frac{1}{\sqrt{2}} + u_{O2}\right)^2} - 1 \right]^2
$$

$$
+ 2\left[\sqrt{\left(\frac{1}{\sqrt{2}} + u_1\right)^2 + \left(\frac{1}{\sqrt{2}} - u_{O1}\right)^2} - 1 \right]^2
$$

$$
+ 2\left[\sqrt{\left(\frac{1}{\sqrt{2}} + u_2\right)^2 + \left(\frac{1}{\sqrt{2}} - u_{O2}\right)^2} - 1 \right]^2
$$

$$
+ \left[\sqrt{1 + (u_1 - u_{O1})^2} - 1 \right]^2 + \left[\sqrt{1 + (u_2 - u_{O2})^2} - 1 \right]^2
$$

$$
\left. + \left[\sqrt{1 + (u_1 + u_{O2})^2} - 1 \right]^2 + \left[\sqrt{1 + (u_2 + u_{O1})^2} - 1 \right]^2 \right\},
$$

$$(9)$$

where the lattice constant of the cubic unit cell is set to 4, so that the lengths of Fe(A)-O and Fe(B)-O bonds without any distortion are 3/4 and 1, respectively. $\mathcal{F}_{BD}$ describes the instability toward the BD state along each chain as the temperature decreases, discussed in Sec. II.

In Fig. 7, $\mathcal{F}$ as a function of (u_1, u_2) is plotted for the optimized positions of the Fe(A) and O ions, obtained by minimizing it numerically by varying other variables u_{Ax}, u_{Ay}, u_{Az}, u_{O1}, and u_{O2}. It is plotted for two sets of elastic constants (a) $K_A = 0.1, K_B = 0.3$ and (b) $K_A = 0.5, K_B = 0.3$ at several temperatures. Above T_c, the shape of the parabolic curvature becomes deeper as T_c is approached, almost symmetrically along $u_1 = u_2$ and $u_1 = -u_2$ suggesting that the fluctuations of both in phase and antiphase BD states develop. Below T_c, for the parameters in Fig. 7(a), the minimum of the free energy appears along $u_1 = u_2$, that is, the in phase BD state is stabilized, while in Fig. 7(b) the mimimum is along $u_1 = -u_2$ which means that the antiphase BD state is realized. Note that the phase transition is a second-order one.
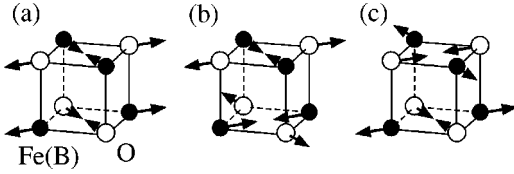
FIG. 8. Schematic view of the lattice displacements in the Fe(B)-O cubes connecting adjacent Fe(B)$_2$O$_4$ layers when the BD state is stabilized. In the in phase BD pattern only the displacement pattern (a) is realized, while in the antiphase BD pattern (a), (b) and (c) are realized with a ratio of 2:1:1.

The stability of these BD patterns can be understood as follows. In the presence of an in phase BD pattern, all the Fe(B)$_4$O$_4$ cubes,[25] connecting the Fe(B)$_2$O$_4$ xy planes, show ionic displacements as shown in Fig. 8(a), where all the interlayer Fe(B)-O pairs move in the same direction, providing small $\Delta u_{B\text{-}O}$'s. Thus the lattice elastic energy of the Fe(B)-O bonds, $\mathcal{E}_{B\text{lat}}$, should be the lowest for the in-phase BD states with such configuration, compared to other BD patterns containing cubes as shown in Figs. 8(b) and 8(c), with both Fe(B) pairs forming dimers or both being interdimer Fe(B) pairs, respectively. For example, the antiphase BD shows all of these three kinds of cubes, realized with a ratio of 2:1:1 in order, thus costing higher $\mathcal{E}_{B\text{lat}}$ than in-phase BD.

On the other hand, the Fe(A)-O tetrahedra would be quite deformed in the presence of the in phase BD, which is shown in Fig. 9(a), providing a large lattice elastic energy of the Fe(A)-O bonds, $\mathcal{E}_{A\text{lat}}$, while the antiphase BD pattern cause the O ions surrounding the Fe(A) ions to show displacements as in Fig. 9(b), where the cost in $\mathcal{E}_{A\text{lat}}$ will be rather smaller. This is because the motion of the oxygens are in the same direction for the latter pattern, so that the Fe(A) ions can adjust their position to lower $\Delta u_{A\text{-}O}$, as can be seen in Fig. 9(b). To summarize, one can say that $\mathcal{E}_{B\text{lat}}$ favors an in-phase BD state while $\mathcal{E}_{A\text{lat}}$ favors an antiphase one.

These naive discussions are consistent with the above calculation of the Landau-type free energy. There, we have observed that a competition arises between the in phase and antiphase BD states, stabilized for $K_A \lesssim K_B$ and $K_A \gtrsim K_B$, respectively. We propose that the latter is the case in magnetite, since, in general, large deformations are hardly realized in the tetrahedra of oxygen surrounding the A sites of the spinel structure, which may be due to its tight packing compared to the B sites.[26] The importance of such ionic displacement of the O ions surrounding the A sites in determining the electronic properties in the ground state was recently also
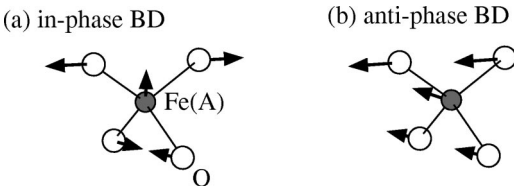
FIG. 9. Schematic view of the displacements in the Fe(A)-O tetrahedra for (a) the in phase BD pattern and (b) the antiphase BD pattern.
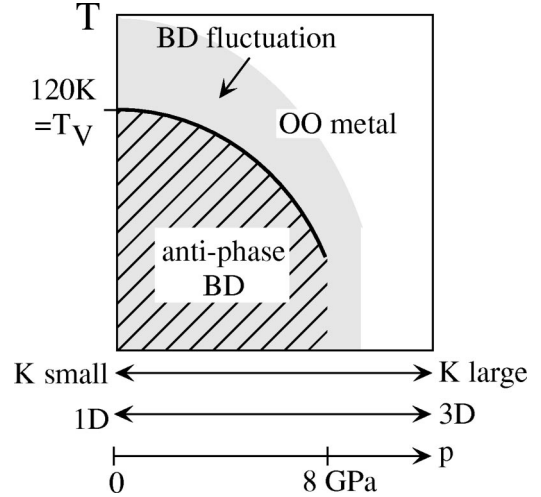
FIG. 10. Schematic phase diagram for magnetite Fe$_3$O$_4$. The OO and BD denotes the orbital-ordered and bond-dimerized states, respectively. The vertical axis is the temperature T, while the horizontal axis can be interpreted either as the pressure p, the "rigidness" of the lattice represented by the lattice constant K, or the effective dimensionality. The bold line is the Verwey transition temperature T_V, varying as a function of such parameters.

pointed out in another spinel compound AlV$_2$O$_4$.[27] This antiphase BD state provides the correct unit cell determined experimentally,[28] as will be discussed below.

IV. COMPARISON WITH EXPERIMENTS

Based on the discussion above, our proposal for the physical properties in magnetite Fe$_3$O$_4$ can be summarized in Fig. 10, which has the following interesting features: the existence of OO in B sites at all temperatures below room temperature, BD fluctuations (both the in phase and the antiphase BD's) above the Verwey transition temperarure T_V, and an antiphase BD stabilized in the insulating phase as a consequence of compensation by the lattice elastic energy of the whole system. These are compared with the known experimental facts in the following.

Below the Verwey transition temperature, the existence of ferro-OO is supported by dielectric measurements showing large anisotropy.[29] Above T_V, in contrast, crystal structure analyses show no evidence of the lowered symmetry from the cubic phase, apparently contradicting our prediction of ferro-OO even in the metallic phase. However, the symmetry in the electronic structure has been pointed out to be lower than the cubic one[30] based on magneto-crystalline anisotropy measurements[31] and on recent resonant x-ray scattering measurements at room temperature,[13] consistent with the OO state.

As for the BD, there is a strong support from a neutron-scattering measurement by Shapiro *et al.*,[32] who observed a *1D correlation* above T_V, not explained by CO but consistent with the present BD picture. This 1D nature of the BD transition can naturally provide an explanation for the critical fluctuation above T_V observed in a large temperature range up to room temperature, such as in the pseudogap structure

of the optical conductivity[33] and in neutron-scattering measurements,[12] where it was actually realized that atomic displacement plays an important role. Moreover, our scenario, that the Verwey transition is a phase transition from OO metal to the coexistent state of OO and BD, explains the entropy change of $\Delta S = R\log2$ per mole of Fe_3O_4 estimated from specific-heat measurements,[34] arising from the degree of freedom for dimerization. This excludes the order-disorder-type CO picture of Ref. 3, predicting $\Delta S = 2R\log2$ as well as simultaneous OO and BD transition with $\Delta S = 2R\log3$ from the orbital degree of freedom.

The crystal structure in the presence of antiphase BD provides the correct unit-cell size below T_V in the actual compound, namely, $\sqrt{2} \times \sqrt{2} \times 2$ of the cubic unit cell above T_V shown in Fig. 1,[28] which is also supported by the double period modulation along the z axis observed in electron diffraction[35] and neutron scattering.[36] Furthermore, the diffusive spot above T_V of the corresponding wave vector $(0,0,\frac{1}{2})$, observed in a neutron-scattering measurement showing a divergent behavior toward T_V,[12] can be assigned to the antiphase BD fluctuation developing above T_V seen in the calculation of Sec. III. On the other hand, the analysis of Yamada *et al.*[37] of their neutron-scattering data above T_V apparently seems to correspond to the in phase fluctuation, where the ionic motions of the $Fe(B)$-O cubes are proposed to be as in Fig. 8(a). This might be the observation of the fluctuation of the in phase BD mode, which is also seen in our calculation, though a long-range order of this mode is not achieved. We have seen that such a competition arises due to the existence of two kinds of elastic energies, $\mathcal{E}_{A\text{lat}}$ and $\mathcal{E}_{B\text{lat}}$, which may be consistent with the experimental findings by Shapiro *et al.* that "two types of interacting dynamical variables are taking part in the neutron scattering."[32]

The observed pressure-induced metallic behavior[16] can be naturally understood, since the pressure should effectively increase the value of K in Eq. (3) [or K_A and K_B in Eqs. (4) and (5)] making the lattice more "rigid," and/or increase the three dimensionality of the system, both expected to destabilize the BD state, which is represented in Fig. 10. This is analogous to the case of spin-Peierls transition, the mapped state of the BD state as mentioned in Sec. II B, known to be destroyed by enhancement in the electron-lattice coupling constant and/or the three dimensionality.[38] We point out the possibility that a three-dimensional BD pattern may be changed under different environments such as pressure and temperature, since there are two competing phases, the in phase and antiphase BD states, as seen in Sec. III. A search for such transitions between these phases under uniaxial pressure is also interesting, since these states are highly anisotropic. Another possibility is that incommensurate phases may be stabilized as a consequence of such competition, as observed in dielectrics $[N(CH_3)_4]_2MCl_4$ (Ref. 39) as well as in CO systems such as perovskite Ni oxides (Ref. 40) and NaV_2O_5,[41] due to competing different states.

One discrepancy between our theory and the experimental

facts is the order of the phase transition: experimentally it is first order, while it is second order in our calculations in Secs. II and III. This discrepancy may be due to the simplified approximation we made for the strucural change as discussed in Sec. III. In an actual compound, the lattice distortion will be more complicated than in our calculation, represented as in Fig. 6, e.g., the lattice distortion of the B sites along the chain should take a period of four sites which is contained in the unit cell, as $(u_a, -u_b, u_c, -u_d, u_a, -u_b, \ldots)$, rather than $(u, -u, u, -u, \ldots)$ as in our calculation. This should make the crystal symmetry of a BD insulating phase lower than that in our calculation, which may lead to a first-order phase transition.[42]

Finally, it is noted that the recent findings of possible charge disproportionation in the B sites by x-ray anomalous scattering[43] does not contradict with our proposal here. The antiphase BD state gives rise to crystallographically independent $Fe(B)$ ions, which should make the charge density on the B sites different, where the amount of charge disproportionation will be not so large but where it can be detectable in a sensitive probe such as x-ray anomalous scattering measurements.

Although we have seen that known experimental facts are practically in agreement with our picture here, further experimental studies are surely necessary for confirmation, especially an accurate determination of the atomic positions below T_V. As for a comparison between theory and experiments on a quantitive level, treatments beyond the mean field may be needed, e.g., for the analysis of the critical fluctuation above T_V observed by different experimental probes mentioned above.

V. CONCLUSION

In conclusion, we have theoretically proposed a model for the mechanism of a Verwey transition in magnetite Fe_3O_4. It is not a charge ordering transition, as has been believed for more than half a century, but a bond dimerization induced by the Peierls instability in a one-dimensional state as a consequence of ferro-orbital ordering due to strong electronic correlation. The actual bond dimerization pattern is predicted to be an antiphase pattern, based on discussions on the lattice elastic energy of the system. This model seems to be able to provide the explanation for the long lasting mystery of the Verwey transition in this compound.

[1] For recent reviews, M. Imada, A. Fujimori, and Y. Tokura, Rev. Mod. Phys. **70**, 1039 (1998), Sec. E.1; N. Tsuda, K. Nasu, A. Fujimori, and K. Shiratori, *Electronic Conduction in Oxides*, 2nd ed.(Springer-Verlag, Berlin, 2000), p. 243.

[2] E. J. W. Verwey, Nature (London) **144**, 327 (1939).

[3] E. J. W. Verwey and P. W. Haayman, Physica (Amsterdam) **8**, 979 (1941); E. J. W. Verwey, P. W. Haayman, and F. C. Romeijn, J. Chem. Phys. **15**, 181 (1947).

[4] J. R. Cullen and E. R. Callen, Phys. Rev. B **7**, 397 (1973).

[5] D. Ihle and B. Lorenz, Philos. Mag. B **42**, 337 (1980).

[6] A. Yanase and K. Shiratori, J. Phys. Soc. Jpn. **53**, 312 (1984).

[7] Z. Zhang and S. Satpathy, Phys. Rev. B **44**, 13 319 (1991).

[8] V. I. Anisimov, I. S. Elfimov, N. Hamada, and K. Terakura, Phys. Rev. B **54**, 4387 (1996).

[9] M. Mizoguchi, J. Phys. Soc. Jpn. **44**, 1512 (1978).

[10] J. M. Zuo, J. C. H. Spence, and W. Petuskey, Phys. Rev. B **42**, 8451 (1990).

[11] P. W. Anderson, Phys. Rev. **102**, 1008 (1956).

[12] Y. Fujii, G. Shirane, and Y. Yamada, Phys. Rev. B **11**, 2036 (1975).

[13] J. García, G. Subías, M. G. Proietti, H. Renevier, Y. Joly, J. L. Hodeau, J. Blasco, M. C. Sánchez, and J. F. Bérar, Phys. Rev. Lett. **85**, 578 (2000).

[14] P. Novak, H. Stepankova, J. Englich, J. Kohout, and V. A. M. Brabers, Phys. Rev. B **61**, 1256 (2000).

[15] J. García, G. Subías, M. G. Proietti, J. Blasco, H. Renevier, J. L. Hodeau, and Y. Joly, Phys. Rev. B **63**, 054110 (2000).

[16] S. Todo, N. Takeshita, T. Kanehara, T. Mori, and N. Môri, J. Appl. Phys. **89**, 7347 (2001).

[17] For reviews, see H. Fukuyama, H. Seo, and H. Kino, Physica B **280**, 462 (2000); H. Fukuyama and H. Seo, J. Phys. Soc. Jpn. **69**, Suppl. B, 144 (2000).

[18] H. Kino and H. Fukuyama, J. Phys. Soc. Jpn. **65**, 2158 (1996); K. Kanoda, Hyperfine Interact. **104**, 235 (1997).

[19] J. Bernasconi, M. J. Rice, W. R. Schneider, and S. Strässler, Phys. Rev. B **12**, 1090 (1975).

[20] K. Mishra, Z. Zhang, and S. Satpathy, J. Appl. Phys. **76**, 15 (1994).

[21] The t_{2g} orbital level in the spinel structure splits into e_g and a_{1g} symmetry combinations, though band-structure calculations show that the octohedral component in the crystal field, at the B site in Fe_3O_4, is so strong that the splitting is negligible (Ref. 7).

[22] J. C. Slater and G. F. Koster, Phys. Rev. **93**, 1498 (1954); W. A. Harrison, *Electronic Structure and the Properties of Solids* (Dover, New York, 1989).

[23] We have repeated the calculation of Mishra *et al.* (Ref. 20), and the value we obtained for V_c was 0.29 eV, smaller than theirs. The difference should be due to the larger number of mesh in our calculation taken for the k integration, though it is not important for the discussion here.

[24] H. Seo and M. Ogata, Phys. Rev. B **64**, 113103 (2001).

[25] Strictly speaking, the Fe(B)-O network is formed not in cubes but in parallelepipeds, though it is approximately cubic in form, so we call them "cubes" in this paper for simplicity.

[26] E. J. W. Verwey and E. L. Heilmann, J. Chem. Phys. **15**, 174 (1947).

[27] K. Matsuno, T. Katsufuji, S. Mori, Y. Moritomo, A. Machida, E. Nishibori, M. Takata, M. Sakata, N. Yamamoto, and H. Takagi, J. Phys. Soc. Jpn. **70**, 1456 (2001).

[28] M. Iizumi, T. F. Koetzle, G. Shirane, S. Chikazumi, M. Matsui, and S. Todo, Acta Crystallogr., Sect. B: Struct. Crystallogr. Cryst. Chem. B **38**, 2121 (1982).

[29] M. Kobayashi, Y. Akishige, and E. Sawaguchi, J. Phys. Soc. Jpn. **55**, 4044 (1986).

[30] K. Siratori and Y. Kino, J. Magn. Magn. Mater. **20**, 87 (1980).

[31] K. Abe, Y. Miyamoto, and S. Chikazumi, J. Phys. Soc. Jpn. **41**, 1894 (1976).

[32] S. M. Shapiro, M. Iizumi, and G. Shirane, Phys. Rev. B **14**, 200 (1976).

[33] S. K. Park, T. Ishikawa, and Y. Tokura, Phys. Rev. B **58**, 3717 (1998).

[34] J. P. Shepherd, J. W. Koenitzer, R. Aragón, C. J. Sandberg, and J. M. Honig, Phys. Rev. B **31**, 1107 (1985).

[35] T. Yamada, K. Suzuki, and S. Chikazumi, Appl. Phys. Lett. **13**, 172 (1968).

[36] E. J. Samuelson, E. J. Bleeker, L. Dobrzynski, and T. Riste, J. Appl. Phys. **39**, 1114 (1968); G. Shirane, S. Chikazumi, J. Akimitsu, K. Chiba, M. Matsui, and Y. Fujii, J. Phys. Soc. Jpn. **39**, 949 (1975).

[37] Y. Yamada, M. Mori, Y. Noda, and M. Iizumi, Solid State Commun. **32**, 827 (1979); Y. Yamada, N. Wakabayashi, and R. M. Nicklow, Phys. Rev. B **21**, 4642 (1980).

[38] E.g., see H. Fukuyama and S. Inagaki, in *Magnetic Properties of Low-Dimensional Systems*, edited by L. M. Falikov and J. L. Morán-López (Springer-Verlag, Berlin, 1986), p. 156.

[39] S. Shimomura, N. Hamaya, and Y. Fujii, Phys. Rev. B **53**, 8975 (1995).

[40] P. Wochner, J. M. Tranquada, D. J. Buttrey, and V. Sachan, Phys. Rev. B **57**, 1066 (1998); H. Yoshizawa, T. Kakeshita, R. Kajimoto, T. Tanabe, T. Katsufuji, and Y. Tokura, *ibid.* **61**, 854 (2000).

[41] K. Ohwada, H. Nakao, H. Nakatogawa, N. Takesue, Y. Fujii, M. Isobe, Y. Ueda, Y. Wakabayashi, and Y. Murakami, J. Phys. Soc. Jpn. **69**, 639 (2000); K. Ohwada, Y. Fujii, N. Takesue, M. Isobe, Y. Ueda, H. Nakao, Y. Wakabayashi, Y. Murakami, K. Ito, Y. Amemiya, H. Fujihisa, K. Aoki, T. Shobu, Y. Noda, and N. Ikeda, Phys. Rev. Lett. **87**, 086402 (2001).

[42] L. D. Landau and E. M. Lifshitz, *Statistical Physics* (Addison-Wesley, Reading, MA, 1958), Chap. XIV.

[43] T. Toyoda, S. Sasaki, and M. Tanaka, Jpn. J. Appl. Phys. **36**, 2247 (1997); Am. Mineral. **84**, 284 (1999).